

# Quantum-mechanical transport properties of $N^+ (^3p)$ and $N^+ (^1D)$ ions in a neutral gas made of helium

S. Lias, L. Aissaoui, M. Bouledroua & K. Alioua

To cite this article: S. Lias, L. Aissaoui, M. Bouledroua & K. Alioua (2019): Quantum-mechanical transport properties of  $N^+ (^3p)$  and  $N^+ (^1D)$  ions in a neutral gas made of helium, Molecular Physics, DOI: [10.1080/00268976.2019.1657601](https://doi.org/10.1080/00268976.2019.1657601)

To link to this article: <https://doi.org/10.1080/00268976.2019.1657601>



Published online: 26 Aug 2019.



Submit your article to this journal [↗](#)





View related articles [↗](#)



View Crossmark data [↗](#)



# Quantum-mechanical transport properties of $N^+$ ( $^3P$ ) and $N^+$ ( $^1D$ ) ions in a neutral gas made of helium

S. Lias <sup>a</sup>, L. Aissaoui<sup>b</sup>, M. Bouledroua<sup>c</sup> and K. Alioua <sup>a,d</sup>

<sup>a</sup>Chérif Messadia University, Souk-Ahras, Algeria; <sup>b</sup>Laboratoire de Physique des Rayonnements et leurs Interactions avec la Matière, Batna 1 University Batna, Algeria; <sup>c</sup>Faculté de Médecine & Laboratoire de Physique des Rayonnements, Badji Mokhtar University, Annaba, Algeria; <sup>d</sup>Laboratoire de Physique de la Matière et du Rayonnement, Chérif Messadia University, Souk-Ahras, Algeria

## ABSTRACT

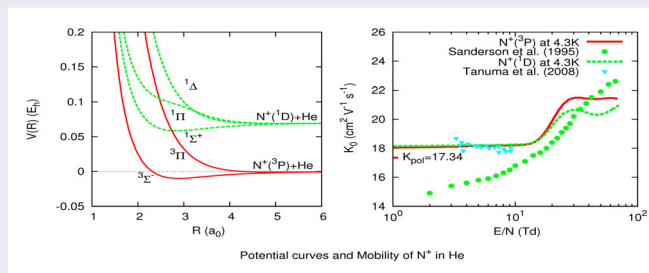
The difficulty to reproduce the measured data by a classic-theoretical calculations of mobility of nitrogen ions  $N^+$  in dilute atom-gas of helium He at low temperatures  $T = 4.3$  and  $77$  K mentioned in the work of Tanuma group [H. Tanuma, S. Matoba and K. Ohtsuki, *Mobility of Ions in Gases*, presented at the Atomic and Molecular Data Application Forum Seminar Aiming at 'Matching the Needs and Seeds of Atomic and Molecular Data' held in National Institute for Fusion Science 17–18 December 2008. < [http://dpsalvia.nifs.ac.jp/amdoc/h201217/Tanuma\\_081217.pdf](http://dpsalvia.nifs.ac.jp/amdoc/h201217/Tanuma_081217.pdf) > ], prompted us to try quantum calculations to minimise this failure. To do this, we have carried out the calculations of the potential-energy curves of the low lying states corresponding to the  $N^+ + He$  ion-atom system using the SA-CASSCF with MRCI *ab initio* methods including the Davidson and BSSE corrections. The transport coefficients of the  $N^+$  ( $^3P$ ) and  $N^+$  ( $^1D$ ) ions in He atom are then carefully determined with special emphasis on the behaviour of the reduced mobility with the ratio  $E/N$  of the electric field and the gas density and try to explain its observed decrease near the value  $E/N \sim 10$  Td.

## ARTICLE HISTORY

Received 23 May 2019  
Accepted 9 August 2019

## KEYWORDS

Chapman–Enskog model; potential-energy curves; transport cross sections; three-temperature theory; mobility and diffusion coefficients



## 1. Introduction

Ionic mobility has been a field of interest for more than a century [1–3]. It continues to these days to be a subject of research intensively studied because of its particular interest in different fields, such as astrophysics, astrochemistry, and many other areas of physics and physical chemistry that require quantitative information regarding the interaction of ionic or neutral, atomic or molecular gas over a wide range of energy and temperature. Indeed, thousands of values, both theoretical and experimental, are now available from an online [4] database where zero-field mobilities as a function of  $T$  are also available, for many systems. Most of the experimental

mobilities were obtained with a drift tube mass spectrometer (DTMS) [5].

Some experiments have recently renewed the interest of this study which focuses on the interaction of various ionised atoms with a buffer gas such as helium He atoms, especially the ions  $O^+$  and  $N^+$  [6],  $C^+$  and  $N^+$  [5], and only  $C^+$  [7] at cold temperatures. Such experiments were carried out by Tanuma and his group using the drift tubes [5]. Experimental measurements on the mobility of nitrogen and carbon ions, in the ground and excited states, moving in a very cold helium gas at 4.3 and 77 K were conducted by Tanuma group [5]. This group found that as the electric field increases, the mobility coefficient

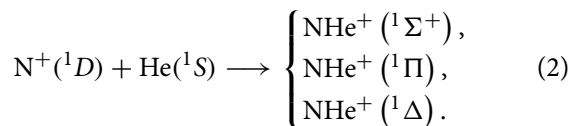
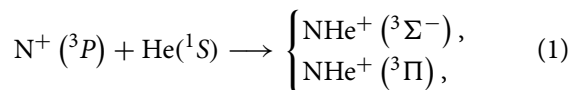
from the polarisation limit decreases to reach a minimum value around 10 Td to increase beyond this value. This behaviour could not be explained by the semi-classical model long used by this group. It has been suggested to use a quantum model of the transport cross sections and a more elaborate theory 3T instead of 2T to find a plausible explanation of the behaviour mobility at very low temperatures.

In the aim of finding a solution to this problem we contribute by this work, which consists in evaluating in a quantum way the mobility of the  $N^+$  ions in He atoms. The first step consists of calculating the interaction potentials corresponding to the  $N^+ - He$  ion-atom which dissociate into  $N^+(^3P) + He(^1S)$  and  $N^+(^1D) + He(^1S)$  by adopting the *state-averaged complete active space self-consistent field* (SA-CASSCF) and the *multireference configuration interaction* (MRCI) levels of theory, including the *Davidson correction* and the *basis-set superposition error* (BSSE). This task is accomplished with MOLPRO package. We therefore compute thermophysical properties by using the Viehland GRAMCHAR Fortran code [8,9] to get in particular the mobility of the  $N^+$  ions at the two temperatures 4.3 and 77 K. The obtained results are compared with theoretical and experimental previous work.

Unless otherwise stated, atomic units (*a.u.*) are used throughout this paper; in particular, energies are in Hartrees ( $E_h$ ) and distances in Bohrs ( $a_0$ ).

## 2. Potential-energy curves

In this section, we expose the *ab initio* methods we used to generate the ion-atom potential-energy curves via which a nitrogen ion, in its ground state  $N^+(^3P)$  or in the first excited state  $N^+(^1D)$ , interact, at thermodynamic equilibrium, with ground-state helium  $He(^1S)$  atoms, along one of the five possible molecular symmetries, namely, the triplet molecular symmetries  $^3\Sigma^-$ , and  $^3\Pi$  corresponding to the  $N^+(^3P) + He(^1S)$  ion-atom pair, and the singlet molecular symmetries  $^1\Sigma^+$ ,  $^1\Pi$ , and  $^1\Delta$ , related to the  $N^+(^1D) + He(^1S)$  system.



In order to determine the potential curves of the above triplet and singlet states, we have chosen the Dunning augmented correlation consistent polarised valence quintuple zeta aug-ccpV5Z basis for both N and He atoms

**Table 1.** Short-range constant parameters (in a.u.) used in the construction of the ground and excited  $NHe^+$  potentials.

Short-range parameters	States				
	$^3\Sigma^-$	$^3\Pi$	$^1\Sigma^+$	$^1\Pi$	$^1\Delta$
$\alpha$	50.821	36.506	47.003	32.469	51.336
$\beta$	3.754	3.313	3.643	3.137	3.763

[10]. We have further performed two level of methods, the first one is the SA-CASSCF followed by the second one MRCI. In the aim to improve the energy, the effect of higher-order excitations of the Davidson correction [11], and the counterpoise method for BSSE [12] are included. The active space is carefully chosen by considering four active electrons distributed among the  $2\sigma$ , and  $2\pi$  orbitals corresponding to  $N(2s; 2p_0; 2p_{\pm})$  of the separated  $N^+$  and He entity, the 4 remaining electrons are considered as frozen. The  $HeN^+$  electronic potential curves are determined in the range of internuclear distances  $1.0 \leq R \leq 29.0$ . All calculations are performed with the quantum chemistry package MOLPRO [13].

The obtained data are therefore linked to the short- and long-range parts of the potential. The short-range region (i.e.  $R \leq 1$ ) is determined by the Born-Mayer formula [14]

$$V_{SR}(R) = \alpha \exp(-\beta R), \quad (3)$$

with  $\alpha$  and  $\beta$  being two parameters to be calculated whose values are shown in Table 1. The long-range region (i.e.  $R \geq 29.0$ ) is performed by the relationship

$$V_{LR}(R) = -\frac{C_4}{R^4} - \frac{C_6}{R^6} - \frac{C_8}{R^8}, \quad (4)$$

with  $C_4$ ,  $C_6$ , and  $C_8$  being the dispersion coefficients which are the half of the dipolar polarisability  $\alpha_d$ , the quadrupole polarisability  $\alpha_q$  and the octupolar polarisability  $\alpha_o$ , of the neutral atom He, respectively. The adopted values of polarisabilities are  $\alpha_d = 1.384$  calculated by Łach *et al.* [15] which is confirmed experimentally by Schmidt *et al.* [16], it is also very close to 1.404 of NIST recommended value and  $\alpha_q = 2.445$  and  $\alpha_o = 10.620$  calculated by Kar and Ho [17].

On the other hand, one can use the dipole polarisability  $\alpha_d$  in determining of the classical polarisation limit  $K_{pol}$  given by

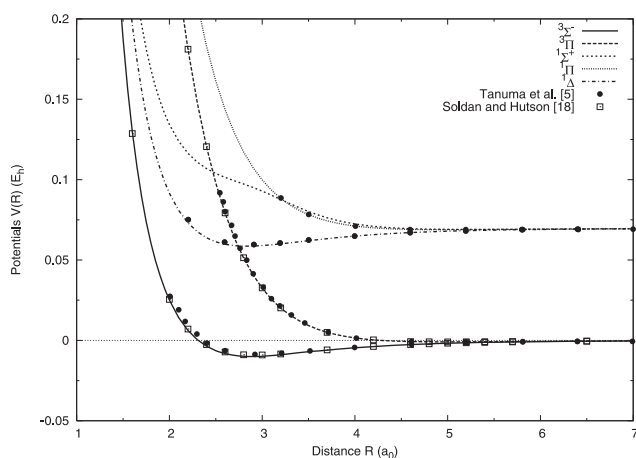
$$K_{pol} = \frac{13.853}{\sqrt{\mu\alpha_d}}, \quad (5)$$

where  $\mu$  being the reduced mass of the ion  $N^+$  and He atom, which leads to  $K_{pol} \simeq 17.35 \text{ cm}^2 \text{ V}^{-1} \text{ s}^{-1}$ .

The potential energy curves we have constructed of the five molecular states  $^3\Sigma^-$ ,  $^3\Pi$ ,  $^1\Sigma^+$ ,  $^1\Pi$ , and  $^1\Delta$  are shown in Figure 1 with those calculated by Tanuma

**Table 2.** Calculated *ab initio* data of the ground and excited NHe<sup>+</sup> states. All the values are given in a.u.

Distance $R(a.u.)$	N <sup>+</sup> ( <sup>3</sup> P) + He( <sup>1</sup> S)		N <sup>+</sup> ( <sup>1</sup> D) + He( <sup>1</sup> S)		
	<sup>3</sup> Σ <sup>-</sup>	<sup>3</sup> Π	<sup>1</sup> Σ <sup>+</sup>	<sup>1</sup> Π	<sup>1</sup> Δ
1.0	-55.708306	-55.570213	-55.599567	-55.420898	-55.638472
1.5	-56.711130	-56.514019	-56.60483	-56.365586	-56.644855
2.0	-56.873688	-56.631673	-56.764735	-56.570721	-56.807446
2.5	-56.905155	-56.800912	-56.795190	-56.737699	-56.837705
3.0	-56.908645	-56.866257	-56.806166	-56.799197	-56.840050
4.0	-56.903352	-56.897207	-56.826556	-56.827867	-56.834123
5.0	-56.900521	-56.899652	-56.829936	-56.830149	-56.831075
6.0	-56.899493	-56.899336	-56.829799	-56.829841	-56.830008
8.0	-56.898942	-56.898924	-56.829410	-56.829416	-56.829435
10.0	-56.898817	-56.898812	-56.829302	-56.829303	-56.829308
12.0	-56.898775	-56.898773	-56.829264	-56.829265	-56.829266

**Figure 1.** The present NHe<sup>+</sup> potential-energy curves corresponding to the molecular states <sup>3</sup>Σ<sup>-</sup>, <sup>3</sup>Π, <sup>1</sup>Σ<sup>+</sup>, <sup>1</sup>Π, and <sup>1</sup>Δ. They are presented and compared with the calculated data of Tanuma *et al.* [5] and Soldán and Hutson [18].

*et al.* [5] and Soldán and Hutson [18]. Where we have chose the value 1.899 eV of the asymptotic separation recommended by NIST [19]. Which are close the 1.9 eV, measured by Tanuma *et al.* [5]. and some of their data points are reported from  $R = 1$  to  $R = 12$  in Table 2

The well-known spectroscopic constants namely, the potential well depth  $D_e$  and the equilibrium distance  $R_e$ , are tabulated in Table 3. They are also compared with experimental and theoretical data when available. For the constants of the <sup>3</sup>Σ<sup>-</sup> and <sup>3</sup>Π states, we can show a concordance with the results of Soldán and Hutson [18] and slightly difference with the theoretical values of Gu *et al.* [20]. Besides, the values of  $D_e$  and  $R_e$  for the three <sup>1</sup>Σ<sup>+</sup>, <sup>1</sup>Π, and <sup>1</sup>Δ states are in excellent agreement with that of Gu *et al.* [20]. We also give in Table 4 the rotationless-vibrational energy levels of all states. As we can see the <sup>3</sup>Σ<sup>-</sup>, <sup>3</sup>Π, <sup>1</sup>Σ<sup>+</sup>, <sup>1</sup>Π, and <sup>1</sup>Δ states hold 12, 6, 6, 6, and 13 vibrational levels, respectively. The above spectroscopic constants and vibrational levels have been determined by using, with slight modifications, the FORTRAN package Level 7.4 written by Le Roy [21].

**Table 3.** Spectroscopic constants of the ground and excited NHe<sup>+</sup> potentials compared with published experimental and theoretical values.

States	$D_e$ (cm <sup>-1</sup> )	$R_e$ (a <sub>0</sub> )	Refs.
<sup>3</sup> Σ <sup>-</sup>	2202.42	2.898	This work
	1435	3.305	[22]
	1414	3.058	[20]
	1954	2.922	[18]
	1563	3.016	[23]
<sup>3</sup> Π	199.70	4.993	This work
		5.444	[20]
	192	4.985	[18]
	177.44	5.131	[23]
<sup>1</sup> Σ <sup>+</sup>	162.91	5.223	This work
	182.17	5.369	[20]
<sup>1</sup> Π	201.09	4.994	This work
	182.14	5.369	[20]
<sup>1</sup> Δ	2458.22	2.831	This work
	1748	2.970	[20]

**Table 4.** Rotationless-vibrational energy levels  $E(v, J = 0)$  (in cm<sup>-1</sup>) of the ground and excited NHe<sup>+</sup> molecular states.

Vibrational level $v$	N <sup>+</sup> ( <sup>3</sup> P) + He ( <sup>1</sup> S)		N <sup>+</sup> ( <sup>1</sup> D) + He ( <sup>1</sup> S)		
	<sup>3</sup> Σ <sup>-</sup>	<sup>3</sup> Π	<sup>1</sup> Σ <sup>+</sup>	<sup>1</sup> Π	<sup>1</sup> Δ
0	-1962.4875	-146.8677	-117.3481	-149.2058	-2202.2212
1	-1514.6953	-70.0707	-52.4771	-72.3900	-1731.2400
2	-1127.4278	-27.4355	-18.7723	-28.2517	-1320.5081
3	-810.3508	-8.0772	-4.7826	-8.3943	-969.6857
4	-550.7256	-1.4076	-0.6096	-1.4941	-678.2517
5	-348.4478	-0.0574	-0.0053	-0.0657	-445.2749
6	-200.2961				-268.9906
7	-101.4431				-145.8854
8	-43.6326				-68.1906
9	-14.8978				-26.1772
10	-3.4462				-7.4977
11	-0.3395				-1.2349
12					-0.0407

### 3. Transport properties

One we have determined the interaction potential energy curves, corresponding to the five molecular states <sup>3</sup>Σ<sup>-</sup>, <sup>3</sup>Π, <sup>1</sup>Σ<sup>+</sup>, <sup>1</sup>Π, and <sup>1</sup>Δ of the ground and excited states of the NHe<sup>+</sup> system, which their reliability are proved and their quality are assessed. We can therefore

use them to determine the transport properties of the  $N^+$  ion evolving in a bath of He atoms. We are particularly interested by the quantum evaluation of the diffusion coefficients and the mobility which dependent strongly on elastic phase shifts.

### 3.1. Phase shifts

Once the potential energy are carefully determined one can easily solve numerically the radial wave equation that governs the motion of the elastic scattered  $N^+$  ion by He atom, given by

$$\frac{d_l^2 \Phi_l(R)}{d^2 R} + \left[ k^2 - \frac{2\mu}{\hbar^2} V(R) - \frac{l(l+1)}{R^2} \right] \Phi_l(R) = 0, \quad (6)$$

where  $k$ ,  $\mu$ , and  $V(R)$  are the wave number, the reduced mass, the interaction potential between the colliding species at internuclear separation  $R$ , respectively. The energy  $\epsilon$  of relative motion is given by

$$\epsilon = \frac{\hbar^2 k^2}{2\mu}, \quad (7)$$

In order to determine the energy-dependent elastic phase shifts  $\eta_l$  we must forced the partial wave functions  $\Phi_l(R)$ , solution of Equation (6), to behave at large  $R$  like

$$\Phi_l(R) \underset{R \rightarrow \infty}{\sim} \sin \left( kR - \frac{l}{2}\pi + \eta_l \right), \quad (8)$$

which are employed in the quantal computation of the transport cross sections. One may notice that for large values of the angular momentum  $l$ , the phase shifts  $\eta_l(\epsilon)$  can be approximated in the semiclassical treatment [24,25] by

$$\eta_l \approx -\mu \int_{\frac{1}{k}(l+\frac{1}{2})}^{\infty} \frac{V(R)}{\sqrt{(kR)^2 - (l+1/2)^2}} R dR. \quad (9)$$

### 3.2. Diffusion cross sections

The accuracy of the phase shifts are so important for the determination of the required quantal transport cross sections. The quantal mass-transport cross sections, also known as the diffusion cross sections  $Q_d(\epsilon)$  are expressed by [2]

$$Q_d(\epsilon) = \frac{4\pi}{k^2} \sum_{l=0}^{\infty} (l+1) \sin^2(\eta_l - \eta_{l+1}). \quad (10)$$

One can mention the exact knowledge of the phase shifts  $\eta_l(\epsilon)$  at a given energy  $\epsilon$  for a set of angular momentum  $l$  for each molecular state leads exactly to the quantal cross section  $Q_d(\epsilon)$ .

The left graphs of Figure 2, illustrate the behaviour of the individual quantal diffusion cross sections  $Q_d(\epsilon)$  of the  $^3\Sigma^-$ ,  $^3\Pi$  states relative to  $N^+(^3P) + He(^1S)$  system, and  $^1\Sigma^+$ ,  $^1\Pi$ , and  $^1\Delta$  states relative to  $N^+(^1D) + He(^1S)$  system, at low energy  $\epsilon$ , where the quantum effects are important. These cross sections have some undulations with regular resonances peaks. As indicated in the references [2,5], the general behaviour of the transport cross sections depends closely on the depth  $D_e$  of the interaction potential considered, and their decrease becomes smooth and sharp beyond the corresponding energies to the values of this depth. In particular, since the molecular state curve  $^3\Sigma^-$  represents the deepest potential of the ground state  $N^+(^3P)He$ , the slope change occurs, as showed in the right graphs of Figure 2, at the highest energy higher than  $10^{-1}E_h$  and the curves in the right panel of the  $^1\Delta$  state represents the deepest potential of the  $N^+(^1D)He$  with effectively a steepness of slope which occurs at the highest energy higher than  $10^{-1}E_h$ . In addition, if  $Q_{jd}(\epsilon)$  is the mass transfer cross section for the individual state, then the average transport cross sections are expressed as [5]:

$$\bar{Q}(\epsilon) = \frac{\sum_j g_j Q_j}{\sum_j g_j}, \quad (11)$$

where  $g_j$  is the multiplicity of the state  $j$

$$\begin{cases} g = 1 \text{ for } \Sigma \text{ state,} \\ g = 2 \text{ for } \Pi \text{ and } \Delta \text{ states.} \end{cases} \quad (12)$$

In our case, the average diffusion cross sections  $\bar{Q}_d(\epsilon)$  for the two  $^3\Sigma^-$  and  $^3\Pi$  states relative to the diffusion of  $N^+(^3P)$  in He, and for the three  $^1\Sigma^+$ ,  $^1\Pi$ , and  $^1\Delta$  states relative to the move of  $N^+(^1D)$  through He are given by the expressions

$$\bar{Q}_d(\epsilon) = \frac{1}{3}Q_d^\Sigma + \frac{2}{3}Q_d^\Pi \quad (13)$$

and

$$\bar{Q}_d(\epsilon) = \frac{1}{5}Q_d^\Sigma + \frac{2}{5}Q_d^\Pi + \frac{2}{5}Q_d^\Delta, \quad (14)$$

respectively. These average cross sections  $\bar{Q}_d(\epsilon)$  are illustrated in Figure 2 which they will serve to determine the diffusion coefficients and mobility. It is only in the first approximation of the kinetic theory that the quantal momentum-transfer cross section is the most important one. This approximation is accurate within 0.5% at least for 330 of the 332 systems examined by Viehland *et al.* [26]

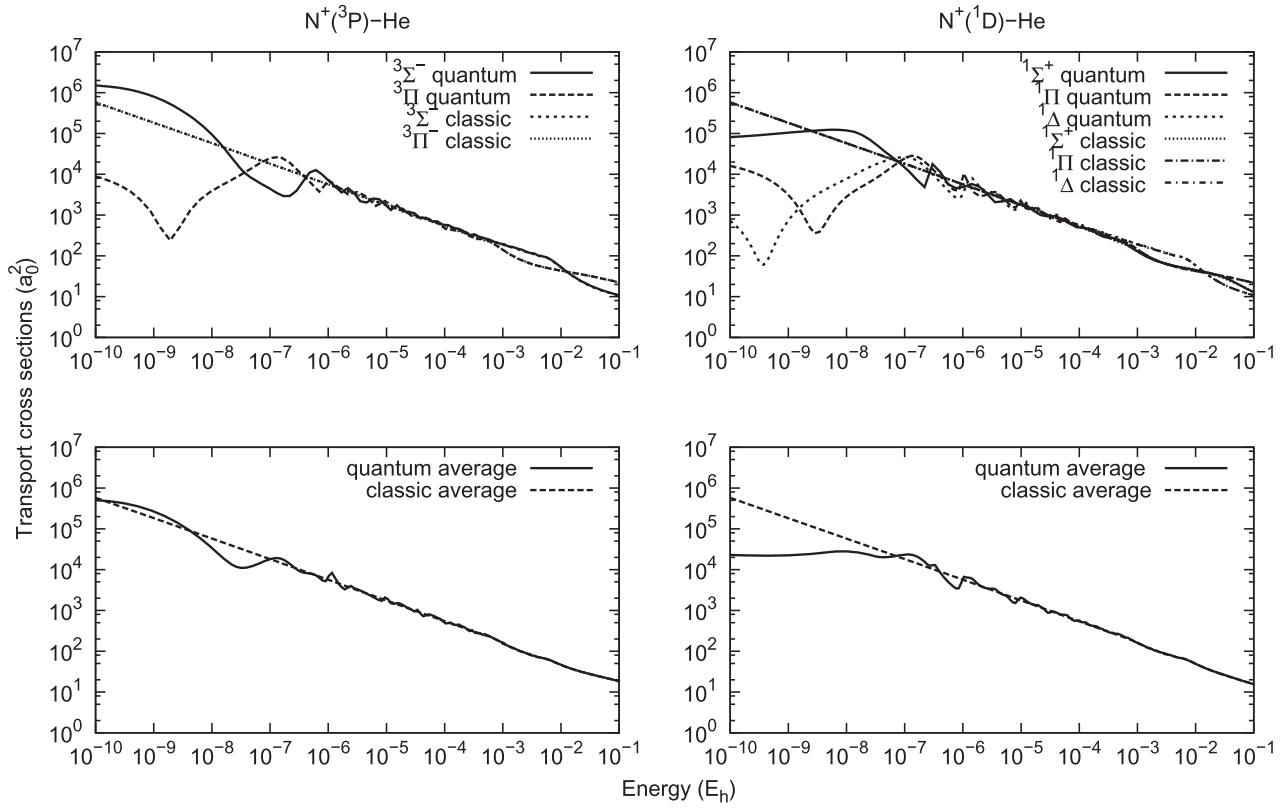


**Figure 2.** Representation of the diffusion cross sections and their average versus the relative colliding energy corresponding to the  $N^+(^3P) + \text{He}$  and  $N^+(^1D) + \text{He}$  systems.

### 3.3. The diffusion coefficients and mobility

The mean transport cross sections should allow the determination of the temperature-dependent diffusion coefficients. According to the Chapman–Enskog model [27]. The diffusion coefficients are defined as

$$D(T) = \frac{3}{16n} \sqrt{\frac{2\pi k_B T}{\mu}} \frac{1}{\Omega^{(1,1)}(T)}, \quad (15)$$

which depend on the collision integral of the diffusion expressed [24] by

$$\Omega^{(1,1)}(T) = \frac{1}{2(k_B T)^3} \int_0^\infty \epsilon^2 \bar{Q}_d(\epsilon) \exp\left(-\frac{\epsilon}{k_B T}\right) d\epsilon, \quad (16)$$

where  $k_B$  denotes the Boltzmann constant and  $n$  is the number of the density of the helium gas. Assuming the case of the low density of the buffer gas, the ideal gas law  $p = nk_B T$  can be applied to the system at hand.

In addition, the null field mobility  $K(T)$  of  $N^+$  ions in the helium buffer gas, is related to the diffusion coefficient  $D(T)$  by the relation [24]

$$K(T) = \frac{q}{k_B T} D(T), \quad (17)$$

where  $q$  being the electric charge of the ion. Usually, we use the reduced mobility  $K_0$  defined by the formula

$$K_0(T) = \left(\frac{p}{760}\right) \left(\frac{273.15}{T}\right) K(T), \quad (18)$$

where, in this special case, the pressure  $p$  and the temperature  $T$  are measured in torr and in kelvins, respectively.

The results of the diffusion coefficient  $D(T)$ , and the reduced mobility  $K_0$ , for  $p = 0.250$  torr and  $T = 299$  K, are given in Table 5. In particular, The theoretical ground state results of  $N^+(^3P) \text{He}$ , are compared to the experimental measurements of Fahey *et al.* [28] see Table 5. It seems to indicate that the present results of  $pD$  for the  $^1D$  state are in closer agreement with the experimental results of Fahey *et al.* [28] than are the present results for the  $^3P$  state which differs only by 4%.

### 3.4. Calculation details of mobility

Because of the relative simplicity of calculating cross sections for closed shells systems, most studies of ion transport kinetic theory have involved alkali metal cations with buffer inert gases. However, there are few theoretical studies, published in the literature, on open-shells systems such as  $N^+$ ,  $C^+$ , and the  $O^+$  of nitrogen, carbon and

**Table 5.** Zero-field reduced mobilities  $K_0$  and diffusion coefficients  $D$  times the buffer gas pressure  $p = 0.250$  torr and number density  $N$  for  $N^+$  ions moving in He at  $T = 299$  K.

Coefficients	$N^+(^3P)$ in He		$N^+(^1D)$ in He
	This work	Fahey <i>et al.</i> [28]	This work
$pD(\text{cm}^2 \text{ torr s}^{-1})$	452	434	436
$ND(10^{19} \text{ cm}^{-1} \text{ s}^{-1})$	1.46	1.41	1.41
$K_0(\text{cm}^2 \text{ V}^{-1} \text{ s}^{-1})$	21.15	$20.5 \pm 1.0$	20.40

Note: The ground-state results are compared with data from Fahey *et al.* [28].

oxygen [29–31], and other experimental works [5,6,32]. Similarly, for our  $N\text{He}^+$  diatomic system, there are some experimental studies, published at different temperatures [23,28,33–36] and a recent experimental study that treats the ion mobility of the  $N^+$  in dilute gas of He atom using a very low temperature drift mass spectrometer at 4.3 and 77 K. In their published works [5], Tanuma and his coworkers suggest improving the calculations using interaction potentials and higher-level kinetic theory. Accordingly, we intend to use the 3T theory and the quantal transport cross sections calculated above to determine the mobility of  $N^+$  in He. On the other hand, we have used a database [4], an open access collection website, available for viewing and downloading electron scattering and cross-sections ions, swarm parameters (mobility, diffusion coefficient, etc.), for comparisons.

Following the same calculation procedure already used for the quantal calculation of transport cross sections [37–40], we inject the average cross sections of the transport  $\bar{Q}_d(\epsilon)$  as a function of the energy  $\epsilon$ , relative to the  $N^+(^3P) - \text{He}$ , and  $N^+(^1D) - \text{He}$  systems in the GC.FOR code of Viehland [9,41] and applying the 3T theory [2], for the calculation of mobility in a non-zero field  $E$ . This code, which is based on the Gram–Charlier series [8], uses the cross sections in three distinct energy regions

$$\epsilon_{\min} \leq \epsilon < \epsilon_c \quad (19)$$

$$\epsilon_c \leq \epsilon < 3\epsilon_c \quad (20)$$

$$3\epsilon_c \leq \epsilon \leq \epsilon_{\max}, \quad (21)$$

where  $\epsilon_c$  is the critical energy when the orbitings occur, which is determined in a range of  $10^{-12} \leq \epsilon < 10^{-1}$  corresponding to roughly to the temperature range  $10^{-9} \leq T < 10^{+2}$  K.

These cross sections are given by a finite sum of Chebyshev polynomials  $\tilde{T}_i[\zeta(\epsilon)]$ , called the Chebyshev coefficients  $a_i$

$$a_i = \frac{2}{N} \sum_{k=0}^N \tilde{T}_i \left[ \cos \left( \frac{k\pi}{N} \right) \log \{ \bar{Q}_d(\epsilon) \} \right] \quad (22)$$

$$\log \{ \bar{Q}_d(\epsilon) \} = \sum_{i=0}^N a_i \tilde{T}_i[\zeta(\epsilon)] \quad (23)$$

$$\zeta(\epsilon) = \frac{2 \log(\epsilon) - \log(\epsilon_{\max}) - \log(\epsilon_{\min})}{\log(\epsilon_{\max}) - \log(\epsilon_{\min})}, \quad (24)$$

where the sign  $i$  above the Chebyshev polynomials  $\tilde{T}_i$  indicates, the first and the last term of its sum.

## 4. Results and discussion

Before to calculate the mobility  $K$  relative to the ground  $N^+(^3P)$  and excited  $N^+(^1D)$  states of nitrogen  $N^+$  in helium He, at two low temperatures 4.3 and 77 K, applying the three-temperatures theory 3 T, we anticipate to treat reduced mobility  $K_0$  at the room temperature  $T = 299$  K of ground and excited  $N^+$  ions in helium He and finally at the temperatures of interest 4.3 and 77 K.

The obtained results of the reduced mobility  $K_0$  corresponding to the  $N^+(^3P) + \text{He}$  at temperature  $T = 299$  K are presented as a function of the ratio  $E/N$  of the electric field strength to the gas number density in Figure 3(a). A comparisons are made with a set of theoretical and experimental data determined at very close temperatures [20,23,28,33,35,36]. As the ratio  $E/N$  goes to zero, the curves show in particular that the value of the lower limits of the reduced mobilities agree quite well with the value  $20.5 \pm 1.0 \text{ cm}^2 \text{ V}^{-1} \text{ s}^{-1}$  measured by Fahey *et al.* [28] and with our calculated value  $21.15 \text{ cm}^2 \text{ V}^{-1} \text{ s}^{-1}$  to which our curve tends. When the electric field increases in intensity, the determined mobility of  $N^+(^3P)$  reach a maximum  $K_0 \simeq 21.46 \text{ cm}^2 \text{ V}^{-1} \text{ s}^{-1}$  that lies between 46 and 53 Td, which is believed typical for mobilities in helium as reported by Peska *et al.* [42]. In addition, as already emphasised by Fahey *et al.* [28], the zero-field mobilities in He show they are generally substantially different from the polarisation value  $K_{\text{pol}} \simeq 17.35 \text{ cm}^2 \text{ V}^{-1} \text{ s}^{-1}$ . This fact indicates that the Langevin approximation is a poor one for ions at room temperature in the rather weakly polarisable helium. However, when the temperature of the gas is sufficiently low, i.e.,  $T \rightarrow 0$ , the polarisation limit is theoretically reached [43]. Furthermore, the calculation of the reduced mobility  $K_0$  of the excited  $N^+(^1D)$  in ground helium gas He at the room temperature  $T = 299$  K, presented in Figure 3(b), show that the mobility approaches the value  $K_0 \simeq 21.15 \text{ cm}^2 \text{ V}^{-1} \text{ s}^{-1}$  as the electric field tends to zero. One can pointed out that when the electric field increases in intensity the mobility of  $N^+(^1D)$  reach a maximum that lies between 75 and 95 Td which corresponds to  $K_0 \simeq 21.33 \text{ cm}^2 \text{ V}^{-1} \text{ s}^{-1}$ . Unfortunately, we did not find data in the literature of the excited  $N^+(^1D)$  to an eventual comparison. We have

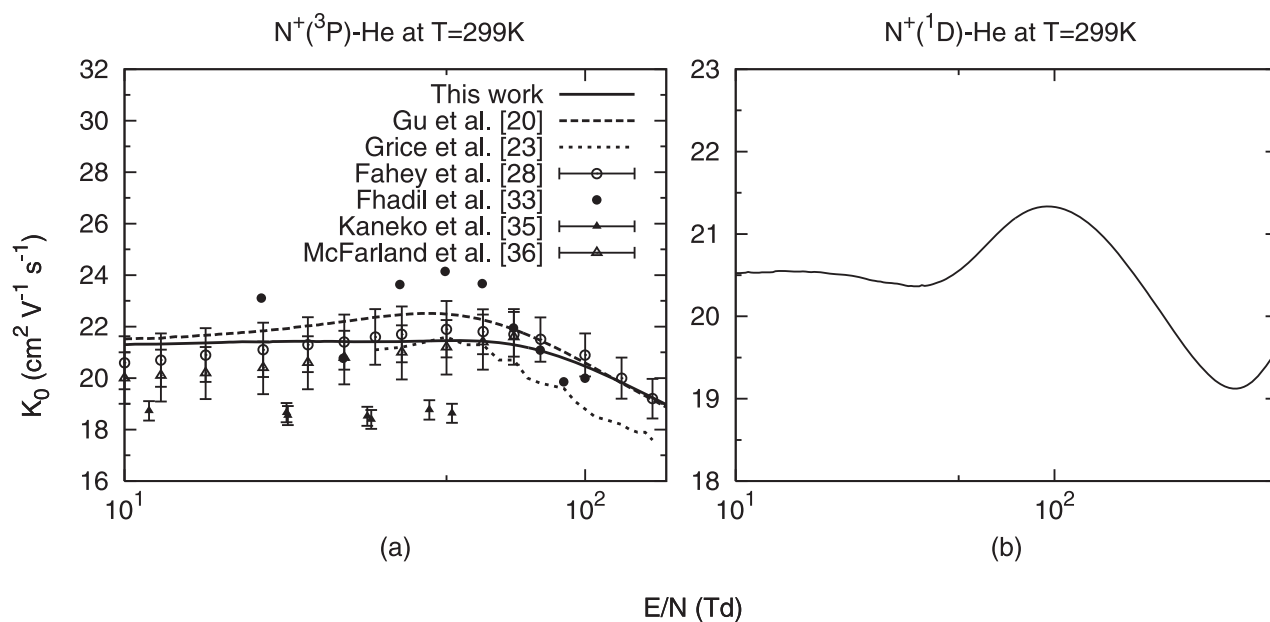


**Figure 3.** Non-zero field mobilities at  $T = 299$  K relative to ground  $N^+(^3P) + He$  and excited  $N^+(^1D) + He$  states. They are compared with theoretical [20,23] and experimental [28,33,35,36] data.

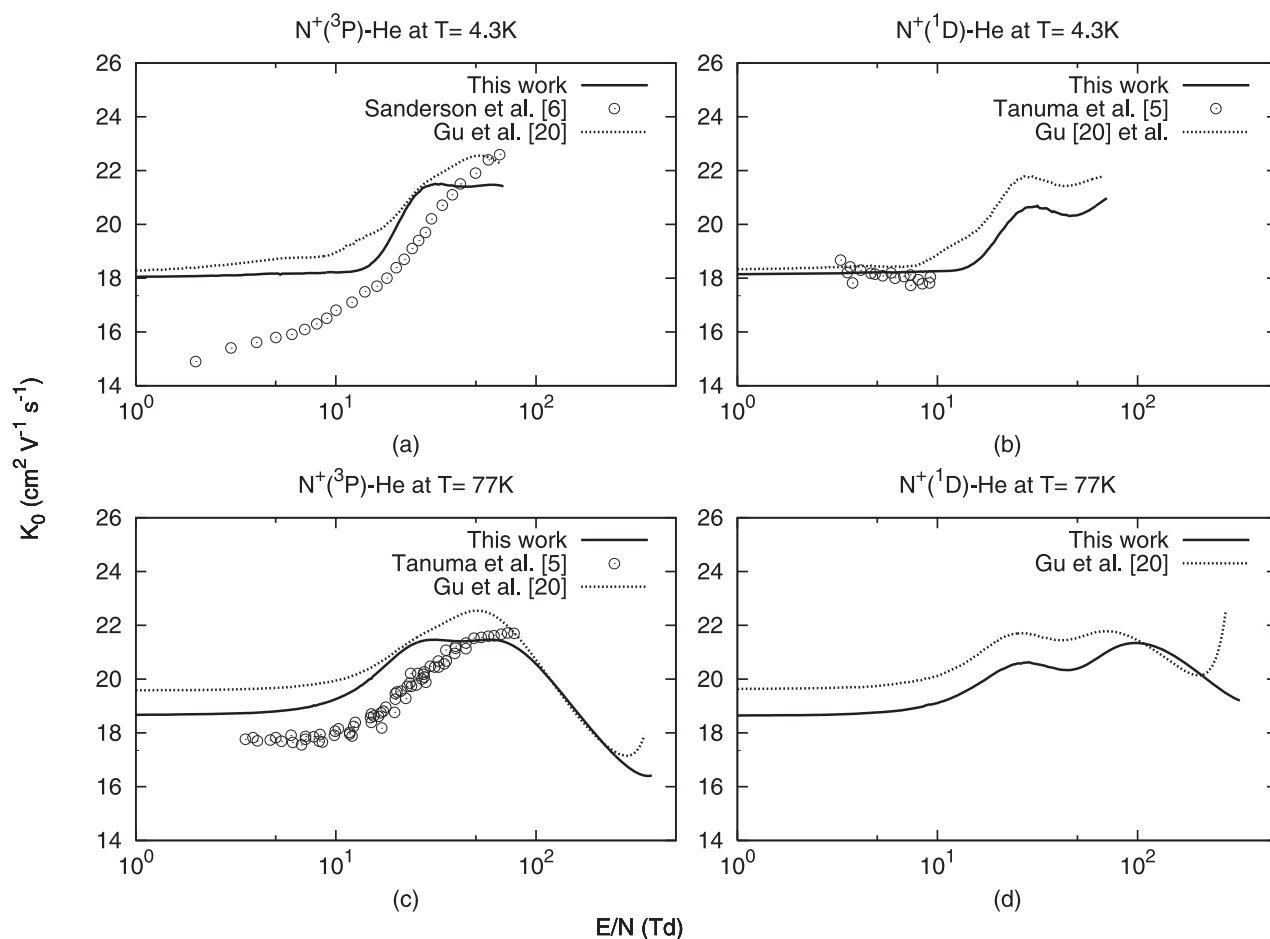


**Figure 4.** Non-zero field mobilities at two distinct temperatures  $T = 4.3$  and  $77$  K relative to ground  $N^+(^3P) + He$  and excited  $N^+(^1D) + He$  states. The results are compared with experimental [5,6] and theoretical [20] data. The polarisation limit is represented with horizontal dotted lines.



further employed the mathematical three-temperature model  $3T$  of Lin *et al.* [44] and Viehland and Lin [45] to generate the mobility of ground and excited  $N^+$  ions in helium He, in terms of the ratio  $E/N$  at very low temperatures namely 4.3 and 77 K. The results are gathered in Figure 4. The graphs in the upper Figure 4(a,b), and in the lower Figure 4(c,d) illustrate the calculations and measurements at the temperatures 4.3 and 77 K, respectively. The solid curves correspond to the results deduced from the use of the present *ab initio* potentials, whereas the dashed lines represent the mobilities obtained with the potentials described by Tanuma *et al.* [5]. The polarisation limit,  $K_{\text{pol}} \simeq 17.35 \text{ cm}^2 \text{ V}^{-1} \text{ s}^{-1}$ , is shown with horizontal dotted lines. All the present calculations are contrasted with the mobility measurements, known with absolute uncertainty of  $0.2 \text{ cm}^2 \text{ V}^{-1} \text{ s}^{-1}$ , performed at the selected temperatures by the TMU group. Otherwise, the Figure 4(a,b) give the reduced mobility coefficients in connection with the ground  $N^+(\text{}^3P)$ , and excited  $N^+(\text{}^1D)$  ions moving into helium He at temperatures 4.3 K, respectively. As the electric field tends to zero, the curves show that the mobility approaches the value  $18.1 \text{ cm}^2 \text{ V}^{-1} \text{ s}^{-1}$ , which is also found from the zero-field analysis based on the Chapman–Enskog model [25,37–40]. For higher values of the ratio  $E/N$ , the experimental data reach their lowest magnitude near 10 Td before they increase again.

On the other hand, the agreement of the present results with the experimental data at 77 K is much better for the curves exhibited in Figure 4(c). Accordingly, this leads us to assume that the accuracy of the quantal collision integrals equation (16) at a higher temperature is good enough. For the same case, as  $E/N \rightarrow 0$ , the reduced mobility appears approaching  $K_0 = 18.66 \text{ cm}^2 \text{ V}^{-1} \text{ s}^{-1}$ , which is in conformity with the zero-field value. In addition we have calculated the most important transport parameters, namely, drift velocity  $v_d$ , reduced mobility  $K_0$ , longitudinal  $T_L$  and transverse  $T_T$  temperatures, and longitudinal  $D_L$  and transverse  $D_T$  diffusion coefficients, that characterise the mobility of  $N^+(\text{}^3P)$  in He, as a function of  $E/N$  at the temperatures 4.3, 77 and 299 K. The obtained results are listed in Tables 6–8. The second column displays the dependence, on  $E/N$ , of the reduced mobility  $K_0$  relevant to the drift movement of excited  $N^+(\text{}^1D)$  ions in helium at 4.3 and 77 K. One may observe in Figure 4(b,d) that, despite the technical complexity of measuring, at low temperatures, the mobility of the excited ionic species in gases, the experimental data are, in this case, only available for 30 Td. The extrapolation of the mobility curves Figure 4(b,d) to the zero-field limits ends at the values  $18.15, 18.63 \text{ cm}^2 \text{ V}^{-1} \text{ s}^{-1}$ , respectively. Once the investigation is complete, it appears that the mobilities are very sensitive to the shape and values of the  $NHe^+$

**Table 6.** Non-zero-field transport properties of *ground*  $N^+$  moving in ground He at 4.3 and 77 K.

$E/N$ Td	$v_d \text{ m s}^{-1}$	$K_0 \text{ cm}^2 \text{ V}^{-1} \text{ s}^{-1}$	$T_L$	$T_T$	$D_L$	$D_T$
			K		$10^{20} \text{ m}^2 \text{ s}^{-1}$	
(a) $T = 4.3 \text{ K}$						
0.017	0.0064	18.04	4.30	4.30	0.17	0.17
1.43	0.52	18.05	5.60	4.81	0.23	0.20
4.96	1.81	18.16	20.14	10.50	0.847	0.44
6.05	2.21	18.16	27.84	13.51	1.171	0.57
8.62	3.15	18.19	52.33	23.09	2.20	0.97
12.76	4.68	18.27	110.36	45.80	4.67	1.93
18.84	7.39	19.51	268.03	107.50	12.11	4.85
24.10	10.15	20.94	501.31	198.79	24.30	9.63
28.18	12.13	21.41	714.15	282.08	35.40	13.98
34.22	14.78	21.49	1059.11	417.07	52.70	20.75
50.02	21.54	21.42	2242.93	880.33	111.23	43.66
60.84	26.25	21.47	3330.78	1306.04	165.57	64.92
68.68	29.57	21.41	4223.08	1655.22	209.42	82.08
(b) $T = 77 \text{ K}$						
0.072	0.0064	18.66	77.00	77.00	3.32	3.32
1.42	0.126	18.67	78.38	77.54	3.38	3.35
4.61	0.411	18.78	91.63	82.72	3.98	3.59
6.04	0.541	18.86	102.33	86.91	4.46	3.79
8.06	0.728	19.03	122.89	94.95	5.41	4.18
18.81	1.848	20.68	372.23	192.53	17.82	9.22
24.12	2.43	21.28	591.00	278.14	29.12	13.70
58.30	5.94	21.46	3131.79	1272.42	155.66	63.24
99.85	9.75	20.56	8299.24	3294.58	395.20	156.88
237.34	19.51	17.30	32,962.3	12,945.9	1320.67	518.69
379.24	29.57	16.41	75,622.6	29,640.0	2874.00	1126.46

Note: The data are computed with the present potentials.

**Table 7.** Non-zero-field transport properties of *excited* N<sup>+</sup> moving in ground He at 4.3 and 77 K.

$E/N\text{Td}$	$v_d\text{m s}^{-1}$	$K_0\text{cm}^2\text{V}^{-1}\text{s}^{-1}$	$T_L$	$T_T$	$D_L$	$D_T$
			K		$10^{20}\text{m}^2\text{s}^{-1}$	
(a) $T = 4.3\text{ K}$						
0.017	0.006	18.15	4.30	4.30	0.18	0.18
0.69	0.25	18.14	4.61	4.42	0.19	0.18
1.02	0.37	18.15	4.97	4.56	0.20	0.19
5.80	2.12	18.21	26.05	12.81	1.09	0.54
6.03	2.20	18.21	27.84	13.51	1.17	.57
8.10	2.97	18.24	46.95	20.99	1.98	0.88
10.07	3.69	18.25	70.24	30.10	2.96	1.27
13.99	5.17	18.40	133.59	54.89	5.69	2.33
17.25	6.56	18.92	212.25	85.67	9.29	3.75
28.66	11.89	20.63	686.60	271.29	32.81	12.96
49.65	20.29	20.33	1992.17	782.17	93.79	36.82
60.80	25.23	20.64	3077.40	1206.88	147.12	57.69
(b) $T = 77\text{ K}$						
0.01	0.001	18.63	77.00	77.00	3.32	3.32
0.70	0.06	18.64	77.33	77.13	3.33	3.32
3.14	0.27	18.68	83.73	79.63	3.62	3.44
6.06	0.541	18.80	102.33	86.91	4.45	3.78
12.03	1.10	19.32	182.42	118.25	8.16	5.29
38.12	1.81	20.41	1902.48	791.60	89.65	37.29
58.34	3.69	20.62	2899.15	1181.39	138.42	56.40
100.12	5.71	21.34	8977.01	3559.82	443.56	175.89
237.05	22.41	19.81	43,468.5	17,057.3	1994.60	782.69
324.14	29.57	19.20	75,622.6	29,640.0	3362.52	1317.93

Note: The data are computed with the present potentials.

**Table 8.** Non-zero field transport properties of *ground* and *excited* N<sup>+</sup> moving in ground He at  $T = 299\text{ K}$ .

$E/N\text{Td}$	$v_d\text{m s}^{-1}$	$K_0\text{cm}^2\text{V}^{-1}\text{s}^{-1}$	$T_L$	$T_T$	$D_L$	$D_T$
			K		$10^{20}\text{m}^2\text{s}^{-1}$	
(a) N <sup>+</sup> ( <sup>3</sup> P) + He( <sup>1</sup> S)						
0.031	0.0016	21.18	299.00	299.00	14.66	14.66
2.47	0.12	21.19	304.36	301.09	14.93	14.77
6.00	0.30	21.22	330.64	311.38	16.24	15.30
12.10	0.62	21.32	428.81	349.81	21.17	17.27
53.09	2.74	21.46	2830.33	1289.58	140.63	64.07
75.32	3.84	21.18	5262.11	2241.20	258.06	109.91
128.55	6.06	19.57	12,640.3	5128.50	572.79	232.39
191.46	8.32	18.04	23,556.7	94,400.39	983.94	392.64
257.24	10.56	17.02	37,707.6	14,938.0	1486.67	588.95
380.95	15.08	16.42	76,608.4	30,160.9	2913.03	1146.87
(b) N <sup>+</sup> ( <sup>1</sup> D) + He( <sup>1</sup> S)						
0.032	0.001	20.48	299.00	299.00	14.17	14.28
2.56	0.12	20.48	304.36	301.09	14.43	14.28
6.21	0.307	20.50	330.64	311.38	15.69	14.78
12.07	0.59	20.53	418.92	345.93	19.91	16.44
46.57	2.29	20.47	2071.33	992.56	98.17	47.04
75.29	3.84	21.19	5262.11	2241.20	258.17	109.95
94.85	4.87	21.33	8281.86	3422.91	409.09	169.7
128.97	6.56	21.11	14,758.8	5957.53	721.56	291.26
191.24	9.37	20.33	29,795.4	11,841.8	1403.11	557.64
383.17	17.67	19.13	105,055	41,293.0	4653.31	1829.03

Note: The values are computed with the present potentials.

potentials. The calculations revealed in particular that the use, within the three-temperature theory, of the quantal cross sections does not make a notable difference in the results of  $K_0$  if compared to those obtained by Tanuma *et al.* [5]. On the other hand the behaviour of the reduced mobility of N<sup>+</sup>(<sup>3</sup>P) in He at 4.3 K indicates the absence of the decrease towards the value of  $E/N \sim 10\text{ Td}$ , which is observed by the group of Tanuma [5]. We could not

explain this behaviour that seems to come from the fact that we have neglected the spin-orbit effects in our calculations of the potential energy curves. Finally, we must mention that Aissaoui *et al.* [46] have attempted to overcome this problem by including the spin-orbit effects in calculating the potential energy curves to determine the mobility of N<sup>+</sup> ions moving in a helium gas at low temperature.

## 5. Conclusion

We have determined the low lying potential-energy curves of the  $\text{NHe}^+$  system using the SA-CASSCF and MRCI *ab initio* methods including the Davidson and BSSE corrections. We have then performed, quantum-mechanically, the calculations of the momentum-transfer cross sections over a wide energy interval and used them to determine the transport parameters. We have further determined the mobility coefficients of  $\text{N}^+$  ions in He at 4.3 and 77 K temperatures using the three-temperature theory  $3T$ . We have also inspected their behaviour with the ratio  $E/N$ . The agreement has been found reasonably good for the meta-stable  $\text{N}^+(^1D)$  state. Since in Figure 4(a) the mobility of  $\text{N}^+(^3P)$  in He at 4.3 K does not approach the polarisability limit, one should mention that this behaviour is a bit strange as one atomic ions.

## Acknowledgments

In this work, we used the Fortran programs GRAMCHAR.F90 and PC.F90 of Dr Larry A. Viehland of Chatham University, Pittsburgh, USA. The authors are very grateful to him for supplying his codes.

## Disclosure statement

No potential conflict of interest was reported by the authors.

## ORCID

S. Lias  <http://orcid.org/0000-0001-6458-4322>

K. Alioua  <http://orcid.org/0000-0003-2770-0798>

## References

- [1] E.W. McDaniel and E.A. Mason, *The Mobility and Diffusion of Ions in Gases* (Wiley, New York, 1973).
- [2] E.A. Mason and E.W. McDaniel, *Transport Properties of Ions in Gases* (John-Wiley, 1988).
- [3] L.A. Viehland and E.A. Mason, *Ann. Phys.* **91**, 499 (1975).
- [4] <http://fr.lxcat.net>.
- [5] H. Tanuma, S. Matoba and K. Ohtsuki, *Mobility of Ions in Gases*, presented at the Atomic and Molecular Data Application Forum Seminar Aiming at 'Matching the Needs and Seeds of Atomic and Molecular Data' held in National Institute for Fusion Science 17–18 December 2008. < [http://dpsalvia.nifs.ac.jp/amdsoc/h201217/Tanuma\\_081217.pdf](http://dpsalvia.nifs.ac.jp/amdsoc/h201217/Tanuma_081217.pdf) > .
- [6] J. Sanderson, H. Tanuma, N. Kobayashi and Y. Kaneko, *J. Chem. Phys.* **103**, 7098 (1995).
- [7] S. Matoba, H. Tanuma and K. Ohtsuki, *J. Phys. B* **41**, 145205 (2008).
- [8] L.A. Viehland, *Chem. Phys.* **179**, 71 (1994).
- [9] L.A. Viehland (communication privée).
- [10] D.E. Woon and T.H. Dunning, Jr., *J. Chem. Phys.* **100**, 2975 (1994).
- [11] E.R. Davidson and D.W. Silver, *Chem. Phys. Lett.* **53**, 403 (1977).
- [12] S.F. Boys and F. Bernardi, *Mol. Phys.* **19**, 553 (1970).
- [13] H.-J. Werner, P.J. Knowles, R. Lindh, F.R. Manby, M. Schütz, P. Celani, T. Korona, G. Rauhut, R.D. Amos, A. Bernhardsson, A. Berning, D.L. Cooper, M.J.O. Deegan, A.J. Dobbyn, F. Eckert, C. Hampel, G. Hetzer, A.W. Lloyd, S.J. McNicholas, W. Meyer, M.E. Mura, A. Nicklass, Palmieri, R. Pitzer, U. Schumann, H. Stoll, A.J. Stone, R. Tarroni and T. Thorsteinsson, MOLPRO, version 2002.6, a package of *ab initio* programs.
- [14] R.B. Bernstein, *Atom-Molecule Collision Theory* (Plenum Press, New York, 1979).
- [15] G. Lach, B. Jezionski and K. Szalewicz, *Phys. Rev. Lett.* **92**, 233001 (2004).
- [16] J.W. Schmidt, R.M. Gavioso, E.F. May and M.R. Moldover, *Phys. Rev. Lett.* **98**, 254504 (2007).
- [17] S. Kar and Y.K. Ho, *Phys. Rev. A* **80**, 062511 (2009).
- [18] P. Soldán and J.M. Hutson, *J. Chem. Phys.* **117**, 3109 (2002).
- [19] < [www.physics.nist.gov](http://www.physics.nist.gov) > .
- [20] J-P. Gu, R.J. Buenker, G. Hirsh and M. Kimira, *J. Chem. Phys.* **102**, 7540 (1995).
- [21] R.J. Le Roy, FORTRAN, Level 7.4 program, University of Waterloo, Chemical Physics Research Report (2001).
- [22] G. Frenking, W. Koch, D. Cremer, J. Gauss and J.F. Liebman, *J. Phys. Chem.* **93**, 3397 (1989).
- [23] S.T. Grice, P.W. Harland, J.A. Harrison, R.G.A.R. MacLagan and R.W. Simpson, *Int. J. Mass Spectrom. Ion Processes* **107**, 215 (1991).
- [24] A. Dalgarno, M.R.C. McDowell and A. Williams, *Proc. Phys. Soc. A* **250**, 411 (1958).
- [25] N.F. Mott and H.S.W. Massey, *The Theory of Atomic Collisions* (Oxford University Press, Oxford, 1965).
- [26] L.A. Viehland, A. Lutfullaeva, J. Dashdorj and R. Johnsen, *Int. J. for Ion Mobil. Spectrom.* **20**, 95 (2017).
- [27] M.R. Flannery, in *Atomic, Molecular, and Optical Physics Handbook*, edited by G.W.F. Drake (AIP Press, Woodbury, New York, 1996).
- [28] D.W. Fahey, F.C. Fehsenfeld and D.L. Albritton, *J. Chem. Phys.* **74**, 2080 (1981).
- [29] W.D. Tuttle, R.L. Thorington, L.A. Viehland and T.G. Wright, *Mol. Phys.* **113**, 3767 (2015).
- [30] H.R. Skullerud, M.T. Elford and I. Røeggen, *J. Phys. B* **29**, 1925 (1996).
- [31] H. Helm and M.T. Elford, *J. Phys. B* **11**, 3939 (1978).
- [32] K. Takaya, Y. Hasegawa, T. Koizumi and H. Tanuma, *Int. J. Ion Mobil. Spec.* **19**, 227 (2016).
- [33] H.A. Fhadil, A.T. Numan, T. Shuttleworth and J.B. Hasted, *Int. J. Mass Spectrom. Ion Processes* **65**, 307 (1985).
- [34] R. Jojinsen, *J. Chem. Phys.* **52**, 10 (1969).
- [35] Y. Kaneko, *J. Mass Spectrosc.* **26**, 1 (1978).
- [36] M. McFarland, D.L. Albritton, F.C. Fehsenfeld, E.E. Ferguson and A.L. Schmeltekopf, *J. Chem. Phys.* **59**, 6610 (1973).
- [37] M. Bouledroua, *Phys. Scripta.* **71**, 519 (2005).
- [38] M.T. Bouazza and M. Bouledroua, *Mol. Phys.* **105**, 51 (2007).
- [39] F. Bouchelaghem and M. Bouledroua, *Phys. Chem. Chem. Phys.* **16**, 1875 (2014).
- [40] L. Aissaoui, M. Bouledroua and K. Alioua, *Mol. Phys.* **113**, 3740 (2015).
- [41] A. Yousef, S. Shrestha, L.A. Viehland, E.P.F. Lee, B.R. Gray, V.L. Ayles, T.G. Wright and W.H. Breckenridge, *J. Chem. Phys.* **127**, 154309 (2007).

- [42] K. Peska, G. Sejkora, H. Stori, F. Egger, H. Ramler, M. Kriegel and W. Lindinger, in *3rd Symposium Atomic and Surface Physics*, edited by W. Lindinger, F. Howorka, T.D. Mark, and F. Egger (Institut für Atomphysik der Universität, Innsbruck, 1982).
- [43] L.A. Viehland, *Aust. J. Phys.* **50**, 671 (1997).
- [44] S.L. Lin, L.A. Viehland and E.A. Mason, *Chem. Phys.* **37**, 411 (1979).
- [45] L.A. Viehland and S.L. Lin, *Chem. Phys.* **43**, 135 (1979).
- [46] L. Aissaoui, P.J. Knowles and M. Bouledroua, in progress.